ISSN 2394-3777 (Print)
ISSN 2394-3785 (Online)
Available online at www.ijartet.com

International Journal of Advanced Research Trends in Engineering and Technology (IJARTET)
Vol. 4, Issue 10, October 2017

Peristaltic Transport of a Micropolar Fluid with Nanoparticles in an Inclined Tube with Permeable Walls

K. Maruthi Prasad[1], N. Subadra[*2], M. A. S. Srinivas[3]
[1]Department of Engineering Mathematics, School of Technology, GITAM University, Hyderabad Campus, Hyderabad, Telangana, India-502329.
Email: kaipa_maruthi@yahoo.com
[2]Department of Mathematics, Geethanjali College of Engg.& Tech., Cheeryal (V), Keesara (M), R.R. Dist., Telangana, India-501301.
Email: nemani.subhadra@gmail.com
[3]Department of Mathematics, JNTUH, Kukatpally, Hyderabad, Telangana, India-500085.
Email: massrinivas@gmail.com
* Corresponding author: nemani.subhadra@gmail.com

Abstract: The paper deals with the theoretical investigation of peristaltic transport of a micropolar fluid in an inclined tube with permeable walls. The closed form expressions for velocity, pressure drop, time averaged flux, frictional force and mechanical efficiency have been investigated under the assumptions of low Reynold's number and long wave length. Effects of different physical parameters like micropolar parameter, coupling number, inclination, Brownian motion parameter, thermophoresis parameter, local temperature Grashof number, local nano particle Grashof number, slip parameter on pressure rise, frictional force, mechanical efficiency, temperature profile, nano particle phenomena, heat transfer coefficient, mass transfer coefficient and streamline patterns have been studied. The computational results are presented in graphical form. The present study puts forward an important note that peristaltic transport of a micropolar fluid with nano particles can be considerably controlled by suitably adjusting the parameters of micropolar fluid like micropolar parameter, coupling number, and also the parameters of nano particle like Brownian motion parameter, thermophoresis parameter. The peristaltic transport can also be controlled by slip parameter and inclination.

Keywords: Peristalsis, Micropolar fluid, Nano particles, Brownian motion parameter, Thermophoresis parameter, Mechanical efficiency, Slip Effect.

I. INTRODUCTION

Peristalsis is a mechanism which is involved in transportation of fluids from one place to another due to contraction or expansion of a tube containing fluid. Peristalsis appears to be the major mechanism in many physiological systems and mechanical situations.

Several researchers have investigated peristalsis in both physiological and mechanical situations.[Fung & Yih, (1968), Shapiro et al.,(1969), Devi & Devanathan, (1975), Meijing et al.,(1993), Maruthi Prasad & Radhakrishnamacharya, (2009), Pincombe et al., (1999), Maruthi Prasad et. al.,(2015), Santhosh et al., (2015)].

Nicoll et al., (1946) suggested that peristalsis plays a vital role in circulation of blood. The effects of an endoscope on peristaltic flow of micropolar fluid was investigated by Hayat et al., (2008). The effect of peripheral layer on the peristaltic transport of a micropolar fluid was studied by Maruthi Prasad et al., (2009).

Nano fluid is a fluid containing nano meter sized particles known as nano particles. The nano particles in nano fluids are typically made of metals, carbides, or carbon nano tubes. Nano fluids possess special properties that make them potentially useful in several applications in heat transfer, including microelectronics, pharmaceutical processes, fuel cells and hybrid powered engines.

Choi, (1995), was the pioneer of study of nano fluid technology. Sohail Nadeem et al., (2014) studied Mathematical model for the peristaltic flow of nanofluid through eccentric tubes comprising porous medium. Peristaltic transport of a nano fluid in an inclined tube was studied by Maruthi Prasad et al., (2015). Maruthi Prasad et al., (2015) also studied the peristaltic transport of nanoparticles of micropolar fluid in an inclined tube with heat and mass transfer effect.

ISSN 2394-3777 (Print)
ISSN 2394-3785 (Online)
Available online at www.ijartet.com

International Journal of Advanced Research Trends in Engineering and Technology (IJARTET)
Vol. 4, Issue 10, October 2017

Most of the researchers have done their study using no slip boundary condition at the walls of the vessels. But in physiological systems, the arteries are having permeable nature. It is proved that there must be some amount of slip at permeable walls. Chu & Fang, (2000) studied peristaltic transport in a slip flow. Slip effects on peristaltic transport of power-law fluid through an inclined tube was studied by Abd El Hakeem et al., (2007). Chaube et al., (2010) studied slip effect on peristaltic transport of micropolar fluid. Ayan Sobh, (2012) studied Peristaltic slip flow of a viscoelastic fluid with heat and mass transfer in a tube. Slip effect on the peristaltic flow of a fractional second grade fluid through a cylindrical tube was studied by Rathod et al., (2015). However, study of peristaltic transport of a micropolar fluid in an inclined tube with permeable walls has not been studied.

Motivated by these studies, study of peristaltic transport of a micropolar fluid in an inclined tube with permeable walls under the assumption of long wavelength and low Reynolds number is investigated. The coupled equations of the temperature profile and nano particle phenomena are solved by using homotopy perturbation technique. The analytical solutions of velocity, pressure rise, frictional force, mechanical efficiency and effect of heat and mass transfer are obtained. The effects of various parameters on these flow variables are investigated and depicted graphically.

II. MATHEMATICAL FORMULATION

Consider the peristaltic transport of an incompressible micropolar fluid with nano particles in an inclined tube. The tube is of uniform cross- section of radius 'a' with sinusoidal waves along the boundary of the tube with constant speed c_1, amplitude b and wave length λ. Also suppose that the tube is inclined at an angle α with the horizontal axis. In this account heat transfer along with nano particle phenomena has been considered. Symmetry condition is used on both the temperature and nano particle phenomena at the center of the tube, while the walls of the tube maintain temperature $\overline{T_o}$ *and* nano particle volume fraction $\bar{C}_o$. Cylindrical polar coordinate system $(\bar{R}, \bar{\theta}, \bar{Z})$ is chosen, so that $\bar{Z}$ −axis coincides with the center line of the tube and $\bar{R}$ is transverse to it. Further the flow is assumed to be axisymmetric. The wall deformation due to propagation of an infinite train of peristaltic waves is given by

$$\bar{R} = \bar{h}(\bar{z}, \bar{t}) = a + b\, Sin\, \frac{2\pi}{\lambda}(\bar{Z} - c_1\bar{t}) \qquad (1)$$

Introducing a wave frame $(\bar{r}, \bar{\theta}, \bar{z})$ moving with a velocity c_1 away from the fixed frame $(\bar{R}, \bar{\theta}, \bar{Z})$ by the transformations

$$\bar{r} = \bar{R},\ \ \bar{z} = \bar{Z} - c_1\bar{t},\quad \bar{w} = \bar{W} - c_1,\quad \bar{u} = \bar{U},\quad \bar{\theta} = \bar{\theta} \qquad (2)$$

in which $\bar{U}, \bar{W}$ and $\bar{u}, \bar{w}$ are the velocity components in the radial and axial directions in the fixed and moving frame coordinates respectively.

The governing equations of motion for micropolar fluid flow in the fixed frame are given by (Maruthi Prasad et al., (2010))

$$div\ \bar{w} = 0 \qquad (3)$$

$$\rho(\bar{w}.\nabla\bar{w}) = -\nabla p + K(\nabla \times \bar{w}) + (\mu + K)\nabla^2\bar{w} \qquad (4)$$

$$\rho j(\bar{w}.\nabla\bar{g}) = -2K\bar{g} + K(\nabla \times \bar{w}) - \boldsymbol{\gamma}(\nabla \times \nabla \times \bar{g}) + (\boldsymbol{\alpha} + \boldsymbol{\beta} + \boldsymbol{\gamma})\nabla(\nabla.\bar{g}) \qquad (5)$$

$$(\rho c)_f \frac{d\bar{T}}{dt} = K\nabla^2\bar{T} + (\rho c)_p[D_B\nabla\bar{C}.\nabla\bar{T} + \frac{D_T}{\overline{T_o}}\nabla\bar{T}.\nabla\bar{T}\ ] \qquad (6)$$

$$\frac{d\bar{C}}{dt} = D_B\nabla^2\bar{C} + \left[\frac{D_{\bar{T}}}{\overline{T_o}}\right]\nabla^2\bar{T} \qquad (7)$$

where $\bar{w}$ is the velocity vector, $\bar{g}$ is the micro rotation vector, p is the fluid pressure, ρ *and* j are the fluid density and micro gyration parameters, μ is the viscosity of micro polar fluid, ρ_f is the density of the fluid, ρ_p is the density of the particle, C is the volumetric volume expansion coefficient, $\frac{d}{dt}$ represents the material time derivative, $\bar{C}$ is the nano particle phenomena, D_B is the Brownian diffusion coefficient and $D_{\bar{T}}$ is the thermophoretic diffusion coefficient. The ambient values of $\bar{T} and \bar{C}$ as $\bar{r}$ tend to $\bar{h}$ are denoted by $\overline{T_o}$ and $\overline{C_o}$. $K, \boldsymbol{\alpha}, \boldsymbol{\beta}, \boldsymbol{\gamma}$ are the material constants and satisfy the following inequalities (Eringen, 1965)

$$2\mu + K \geq 0, \qquad K \geq 0,$$

$$3\boldsymbol{\alpha} + \boldsymbol{\beta} + \boldsymbol{\gamma} \geq 0, \qquad \boldsymbol{\gamma} \geq |\boldsymbol{\beta}|$$

Since the flow is axisymmetric, all the variables are independent of θ and hence for this flow,

$$\bar{w} = (u, 0, w),\quad \bar{g} = (0, v_\theta, 0) \quad \&$$

$$\nabla^2 = \left(\frac{\partial^2}{\partial r^2} + \frac{1}{r}\frac{\partial}{\partial r} + \frac{\partial^2}{\partial z^2}\right)$$

Introducing the following non-dimensional quantities

$$r = \frac{\bar{r}}{a}, z = \frac{\bar{z}}{\lambda}, p = \frac{a^2\bar{p}}{\lambda\mu_c c_1}, u = \frac{\lambda\bar{u}}{c_1 a}, w = \frac{\bar{w}}{c_1}, h = \frac{\bar{h}}{a},$$

$$v_\theta = \frac{\overline{v_\theta}}{a^2},\ t = \frac{c_1\bar{t}}{\lambda}, j = \frac{\bar{j}}{a^2}, \theta_t = \frac{\bar{T} - \overline{T_o}}{\overline{T_o}},$$

$$\delta = \frac{a}{\lambda},\ R_e = \frac{2\rho c_1 a}{\mu}, \sigma = \frac{\bar{C} - \overline{C_o}}{\overline{C_o}},\ N_b = \frac{(\rho C)_P D_{\bar{B}}\overline{C_o}}{(\rho C)_f},$$

$$N_t = \frac{(\rho C)_P D_{\bar{T}}\overline{T_o}}{(\rho C)_f \beta}, G_r = \frac{g\beta a^3\overline{T_o}}{\varphi^2}, B_r = \frac{g\beta a^3\overline{C_o}}{\varphi^2}, \varphi^2 = \frac{\mu}{\rho},$$

in which N_b, N_t, G_r and B_r are the Brownian motion parameter, the Thermophoresis parameter, local

ISSN 2394-3777 (Print)
ISSN 2394-3785 (Online)
Available online at www.ijartet.com

International Journal of Advanced Research Trends in Engineering and Technology (IJARTET)
Vol. 4, Issue 10, October 2017

temperature Grashof number and local nano particle Grashof number.

Using the non-dimensional quantities and applying low Reynold's number and long wave length approximations, the equations (7) to (11) are converted to

$$\frac{\partial u}{\partial r}+\frac{u}{r}+\frac{\partial w}{\partial z}=0 \quad (8)$$

$$R_e\delta^3\left(u\frac{\partial u}{\partial r}+w\frac{\partial u}{\partial z}\right)=-\frac{\partial p}{\partial r}+\frac{\delta^2}{1-N}\left(-N\frac{\partial v_\theta}{\partial z}+\frac{\partial^2 u}{\partial r^2}+\frac{1}{r}\frac{\partial u}{\partial r}-\frac{u}{r^2}+\delta^2\frac{\partial^2 u}{\partial z^2}\right)-\frac{cos\alpha}{F} \quad (9)$$

$$R_e\delta\left(u\frac{\partial w}{\partial r}+w\frac{\partial w}{\partial z}\right)=-\frac{\partial p}{\partial z}+\frac{1}{N-1}\left(\frac{N}{r}\frac{\partial}{\partial r}(rv_\theta)+\frac{\partial^2 w}{\partial r^2}+\frac{1}{r}\frac{\partial w}{\partial r}+\delta^2\frac{\partial^2 w}{\partial z^2}\right)+G_r\theta_t+B_r\sigma+\frac{sin\alpha}{F} \quad (10)$$

$$\frac{jR_e\delta(1-N)}{N}\left(u\frac{\partial v_\theta}{\partial r}+w\frac{\partial v_\theta}{\partial z}\right)=-2v_\theta+\left(\delta^2\frac{\partial u}{\partial z}-\frac{\partial w}{\partial r}\right)+\frac{2-N}{m^2}\left[\frac{\partial}{\partial r}\left(\frac{1}{r}\frac{\partial}{\partial r}(rv_\theta)\right)+\delta^2\frac{\partial^2 v_\theta}{\partial z^2}\right] \quad (11)$$

$$\frac{R_e\delta\mu}{2\rho a^2}\overline{T_0}\left(u\frac{\partial\theta_t}{\partial r}+w\frac{\partial\theta_t}{\partial z}\right)=\frac{\overline{T_0}}{a^2}\left(\frac{1}{r}\frac{\partial}{\partial r}\left(r\frac{\partial\theta_t}{\partial r}\right)\right)+\frac{N_b\overline{T_0}}{a^2}\left(\frac{\partial\sigma}{\partial r}\right)\left(\frac{\partial\theta_t}{\partial r}\right)+\frac{N_t}{a^2}\left(\frac{\partial\theta_t}{\partial r}\right)^2 \quad (12)$$

$$\frac{4R_e\mu\overline{C_0}}{\rho a^2}\left(u\frac{\partial\sigma}{\partial r}+w\frac{\partial\sigma}{\partial z}\right)=\frac{(\rho c)_f}{(\rho c)_p}\frac{1}{a^2}\left[N_b\left(\frac{1}{r}\frac{\partial}{\partial r}\left(r\frac{\partial\sigma}{\partial r}\right)\right)+N_t\left(\frac{1}{r}\frac{\partial}{\partial r}\left(r\frac{\partial\theta_t}{\partial r}\right)\right)\right] \quad (13)$$

where $\tau=\frac{(\rho C)_P}{(\rho C)_f}$ is the ratio between the effective heat capacity of the nano particle material and heat capacity of the fluid. Here $N=\frac{K}{\mu+K}$ is the coupling number ($0\le N<1$), $m^2=\frac{a^2K(2\mu+K)}{\gamma(\mu+K)}$ is the micro polar parameter. v_θ is the micro rotation in the θ direction. Here θ_t and σ are the temperature profile and nano particle phenomena of the fluid.

Using the long wave length approximation ($\delta\ll 1$) and low Reynolds number, equations (9) to (13) reduce to

$$\frac{\partial p}{\partial r}=-\frac{cos\alpha}{F} \quad (14)$$

$$\frac{N}{r}\frac{\partial}{\partial r}(rv_\theta)+\frac{\partial^2 w}{\partial r^2}+\frac{1}{r}\frac{\partial w}{\partial r}+(N-1)\frac{sin\alpha}{F}+(N-1)(G_r\theta_t+B_r\sigma)=(N-1)\frac{\partial p}{\partial z} \quad (15)$$

$$2v_\theta+\frac{\partial w}{\partial r}-\frac{2-N}{m^2}\frac{\partial}{\partial r}\left(\frac{1}{r}\frac{\partial}{\partial r}(rv_\theta)\right)=0 \quad (16)$$

$$0=\frac{1}{r}\frac{\partial}{\partial r}\left(r\frac{\partial\theta_t}{\partial r}\right)+N_b\frac{\partial\sigma}{\partial r}\frac{\partial\theta_t}{\partial r}+N_t\left(\frac{\partial\theta_t}{\partial r}\right)^2 \quad (17)$$

$$0=\frac{1}{r}\frac{\partial}{\partial r}\left(r\frac{\partial\sigma}{\partial r}\right)+\frac{N_t}{N_b}\left(\frac{1}{r}\frac{\partial}{\partial r}\left(r\frac{\partial\theta_t}{\partial r}\right)\right) \quad (18)$$

The non-dimensional boundary conditions are

$$\frac{\partial w}{\partial r}=0,\ \frac{\partial\theta_t}{\partial r}=0,\ \frac{\partial\sigma}{\partial r}=0\ at\ r=0 \quad (19)$$

$$w=-k\frac{\partial w}{\partial r},\qquad \theta_t=0,\qquad \sigma=0,\qquad v_\theta=0\ at\ r=h(z)=1+\varepsilon\, sin2\pi z \quad (20)$$

v_θ is finite, w is finite at $r=0$ (21)

where, $\varepsilon\left(=\frac{a}{b}\right)$ is the amplitude ratio.

III. SOLUTION OF THE PROBLEM

The homotopy for the equations (17) and (18) using homotopy perturbation method is

$$H(\zeta,\theta_t)=(1-\zeta)\left[L(\theta_t)-L(\theta_{t_{10}})\right]+\zeta\left[L(\theta_t)+N_b\frac{\partial\sigma}{\partial r}\frac{\partial\theta_t}{\partial r}+N_t\left(\frac{\partial\theta_t}{\partial r}\right)^2\right] \quad (22)$$

$$H(\zeta,\sigma)=(1-\zeta)[L(\sigma)-L(\sigma_{10})]+\zeta\left[L(\sigma)+\frac{N_t}{N_b}\left(\frac{1}{r}\frac{\partial}{\partial r}\left(r\frac{\partial\theta_t}{\partial r}\right)\right)\right] \quad (23)$$

$L=\frac{1}{r}\frac{\partial}{\partial r}\left(r\frac{\partial}{\partial r}\right)$ is taken as linear operator for convenience.

Consider $\theta_{10}(r,z)=\left(\frac{r^2-h^2}{4}\right)$, $\sigma_{10}(r,z)=-\left(\frac{r^2-h^2}{4}\right)$ (24)

as initial guesses which satisfy the boundary conditions.

Define

$$\theta_t(r,z)=\theta_{t_0}+\zeta\theta_{t_1}+\zeta^2\theta_{t_2}+----- \quad (25)$$

$$\sigma(r,z)=\sigma_0+\zeta\sigma_1+\zeta^2\sigma_2+---- \quad (26)$$

Adopting the same procedure as done by Maruthi Prasad et al., (2015) the solution for temperature profile and nano particle phenomena can be written for $\zeta=1$ as

$$\theta_t(r,z)=\left(\frac{r^4-h^4}{64}\right)(N_b-N_t) \quad (27)$$

$$\sigma(r,z)=-\left(\frac{r^2-h^2}{4}\right)\frac{N_t}{N_b} \quad (28)$$

Equation (15) can be written as

$$\frac{1}{r}\frac{\partial}{\partial r}\left[Nrv_\theta+r\frac{\partial w}{\partial r}+\frac{1-N}{2}r^2\frac{dp}{dz}\right]=(1-N)\frac{Sin\,\alpha}{F}+(1-N)G_r\theta_t+(1-N)B_r\sigma \quad (29)$$

Substituting equations (27) and (28) in equation (29), the equation converted to

$$\frac{1}{r}\frac{\partial}{\partial r}\left[Nrv_\theta+r\frac{\partial w}{\partial r}+\frac{1-N}{2}r^2\frac{dp}{dz}\right]=(1-N)\frac{Sin\,\alpha}{F}+(1-N)G_r\left[\left(\frac{r^4-h^4}{64}\right)(N_b-N_t)\right]-(1-N)B_r\left[\left(\frac{r^2-h^2}{4}\right)\frac{N_t}{N_b}\right] \quad (30)$$

Using equation (30) in equation (16), the equation for v_θ is given as

$$\frac{\partial^2 v_\theta}{\partial r^2}+\frac{1}{r}\frac{\partial v_\theta}{\partial r}-\left(m^2+\frac{1}{r^2}\right)v_\theta=m^2\frac{N-1}{2-N}\frac{r}{2}\frac{dp}{dz}+\frac{1-N}{2-N}m^2\frac{r}{2}\frac{Sin\,\alpha}{F}+\frac{1-N}{2-N}m^2\frac{G_r}{64}(N_b-N_t)\left(\frac{r^5}{6}-\frac{rh^4}{2}\right)+\frac{N-1}{2-N}m^2\frac{B_r}{4}\left(\frac{N_t}{N_b}\right)\left(\frac{r^3}{4}-\frac{rh^2}{2}\right) \quad (31)$$

The general solution for equation (31) is

$$v_\theta=c_2(z)I_1(mr)+c_3(z)K_1(mr)+\frac{1-N}{2-N}\frac{r}{2}\frac{dp}{dz}+\frac{N-1}{2-N}\frac{r}{2}\frac{Sin\,\alpha}{F}$$

ISSN 2394-3777 (Print)
ISSN 2394-3785 (Online)
Available online at www.ijartet.com

International Journal of Advanced Research Trends in Engineering and Technology (IJARTET)
Vol. 4, Issue 10, October 2017

$$+\frac{N-1}{2-N}\,G_r(N_b-N_t)\left(\frac{r}{2m^4}-\frac{rh^4}{128}+\frac{r^3}{16m^2}+\frac{r^5}{384}\right)+\frac{1-N}{2-N}B_r\frac{N_t}{N_b}\left(\frac{r}{2m^2}-\frac{rh^2}{8}+\frac{r^3}{16}\right) \quad (32)$$

where $I_1(mr)$ and $K_1(mr)$ are modified Bessel functions of first and second order respectively.

Substituting equation (32) in equation (30), using the boundary conditions (19)-(21) and solving for w, the equation for velocity is obtained as

$$w=\frac{dp}{dz}\left(A\frac{h}{2}-\frac{N}{m}\frac{N-1}{2-N}\frac{I_0(mr)}{I_1(mh)}\frac{h}{2}+\frac{N-1}{2-N}\frac{(r^2-h^2)}{2}-\frac{k(N-1)h}{2-N}\right)-\frac{N}{m}\frac{N-1}{2-N}\frac{I_0(mr)}{I_1(mh)}B$$
$$+\frac{1-N}{2-N}\frac{Sin\,\alpha}{F}\left(\frac{r^2}{2}-\frac{h^2}{2}-kh\right)+\frac{1-N}{2-N}G_r(N_b-N_t)\left(\frac{Nr^2}{2m^4}+\frac{Nr^4}{64m^2}-\frac{r^2h^4}{128}+\frac{r^6}{1152}\right)$$
$$+\frac{N-1}{2-N}B_r\left(\frac{N_t}{N_b}\right)\left(\frac{Nr^2}{4m^2}-\frac{r^2h^2}{8}+\frac{r^4}{32}\right)+A.B+C \quad (33)$$

where,

$$A=\frac{N(N-1)}{(2-N)}\frac{mkI_1(mh)-I_0(mh)}{mI_1(mh)}$$

$$B=-\frac{h}{2}\frac{Sin\,\alpha}{F}-G_r(N_b-N_t)\left(\frac{h}{2m^4}-\frac{h^3}{16m^2}-\frac{h^5}{192}\right)+B_r\left(\frac{N_t}{N_b}\right)\left(\frac{h}{2m^2}-\frac{h^3}{16}\right)$$

$$C=\frac{1-N}{2-N}G_r(N_b-N_t)\left(\frac{-kNh}{2m^4}-\frac{kNh^3}{16m^2}+\frac{kh^5}{96}-\frac{Nh^2}{4m^2}-\frac{Nh^4}{64m^4}+\frac{h^6}{144}\right)+\frac{N-1}{2-N}B_r\left(\frac{N_t}{N_b}\right)\left(\frac{-kNh}{4m^2}+\frac{kh^3}{8}-\frac{Nh^2}{4m^2}+\frac{3h^4}{32}\right)$$

The dimension less flux in the moving frame is defined as

$$q=\int_0^h 2rw_z dr \quad (34)$$

Substituting equation (33) in equation (34), the flux and $\frac{dp}{dz}$ are calculated.

The pressure drop over the wavelength ΔP_λ is defined as

$$\Delta P_\lambda=-\int_0^1\frac{dP}{dz}dz. \quad (35)$$

Substituting the expression $\frac{dp}{dz}$ in equation (35), the pressure drop is

$$\Delta P_\lambda=qL_1+L_2 \quad (36)$$

where, $L_1=\int_0^1-\frac{1}{S}\,dz$

$$L_2=2\frac{N}{m}\frac{N-1}{2-N}\int_0^1\frac{Bh}{S}\,dz+\int_0^1(A.B+C)\frac{h^2}{S}\,dz+\frac{1-N}{2-N}\frac{Sin\,\alpha}{F}\int_0^1\left(\frac{h^4}{4}+kh^3\right)\frac{1}{S}\,dz$$
$$+\frac{N-1}{2-N}G_r\,(N_b-N_t)\int_0^1\left[\frac{Nh^4}{8m^4}+\frac{Nh^6}{192m^2}-\frac{17h^8}{4608}\right]\frac{1}{S}\,dz+\frac{1-N}{2-N}B_r\left(\frac{N_t}{N_b}\right)\int_0^1\left[\frac{Nh^4}{4m^2}-\frac{5h^6}{96}\right]\frac{1}{S}\,dz$$

$$S=\frac{Ah^3}{3}+\frac{N}{m}\frac{N-1}{2-N}h^2-\frac{1-N}{2-N}\frac{h^4}{4}-\frac{1-N}{2-N}kh^3$$

Following the analysis of Shapiro et al., (1969), the time averaged flux over a period in the laboratory frame $\bar{Q}$ is given as

$$\bar{Q}=1+\frac{\epsilon^2}{2}+q \quad (37)$$

Substituting equation (36) in equation (37), the time averaged flux is

$$\bar{Q}=1+\frac{\epsilon^2}{2}+\frac{\Delta P_\lambda}{L_1}-\frac{L_2}{L_1} \quad (38)$$

When the micro polar parameter $N\to 0$, i.e. the fluid becomes Newtonian, the expression for the time averaged flux reduces to the corresponding expression for a Newtonian fluid as given by Shapiro et al., (1969).

The dimensionless friction force $\bar{F}$ at the wall is given by

$$\bar{F}=\int_0^1 h^2\left(-\frac{dP}{dz}\right)dz \quad (39)$$

The expression for mechanical efficiency is

$$E=-\frac{\bar{Q}\Delta p}{2\pi\epsilon\left(-\int_0^1\frac{dp}{dz}Sin\,2\pi z\,dz-\frac{\epsilon}{4}\Delta p+\frac{\epsilon}{4}\int_0^1\frac{dp}{dz}Cos\,2\pi z\,dz\right)} \quad (40)$$

The coefficient of heat and mass transfer at the wall is given by

$$Z_\theta(r,z)=\left(\frac{\partial h}{\partial z}\right)\left(\frac{\partial\theta_t}{\partial r}\right) \quad (41)$$

$$Z_\sigma(r,z)=\left(\frac{\partial h}{\partial z}\right)\left(\frac{\partial\sigma}{\partial r}\right) \quad (42)$$

IV. Results And Discussion

The effects of various parameters on pressure rise, time averaged flux, frictional force, heat transfer coefficient and mass transfer coefficient have been computed numerically and the results are presented graphically using Mathematica 9.0 software.

A. *Pressure rise characteristics*

The effects of various parameters like micropolar parameter (m), coupling number (N), inclination (α), Brownian motion parameter (N_b), thermophoresis parameter (N_t), slip parameter (k), local temperature Grashof number (G_r) and local nano particle Grashof number (B_r) on the pressure rise $(-\Delta P_\lambda)$ are shown in figures 1.1-1.8. It is observed from Figs. 1.1, 1.2, 1.3, 1.4 and 1.6 that, pressure rise $(-\Delta P_\lambda)$ decreases with the increase of micropolar parameter (m), coupling number (N), Brownian motion parameter (N_b), thermophoresis parameter (N_t) and with local nano particle Grashof number (B_r). It is noticed from Figs 1.5 and 1.7 that, pressure rise $(-\Delta P_\lambda)$ increases with the increase of local temperature Grashof number (G_r) and with the inclination

ISSN 2394-3777 (Print)
ISSN 2394-3785 (Online)
Available online at www.ijartet.com

International Journal of Advanced Research Trends in Engineering and Technology (IJARTET)
Vol. 4, Issue 10, October 2017

(α). It can be seen from Fig. 1.8 that, the pressure rise ($-\Delta P_\lambda$) decreases with the increase of slip parameter (k) in the region $\bar{Q} \in [0, 0.8]$ and pressure rise ($-\Delta P_\lambda$) increases in the region $\bar{Q} \in [0.8, 1]$. It is interesting to observe that, pressure rise ($-\Delta P_\lambda$) increases with the increase of time averaged flux ($\bar{Q}$) with fixed values of micropolar parameter (m), Brownian motion parameter (N_b), thermophoresis parameter (N_t), local temperature Grashof number (G_r) and with inclination (α). It is also observed from Fig. 1.2 that, pressure rise also increases with the increase of time averaged flux for fixed values of Brownian motion parameter and converges to a particular value.

B. Frictional Force

The effects of various parameters on the frictional force ($\bar{F}$) are shown in figs. 2.1-2.8. It is observed from Figs. 2.1, 2.4, 2.5, 2.6 and 2.7 that, the frictional force ($\bar{F}$) decreases with the increase of micropolar parameter (m), thermophoresis parameter (N_t), local temperature Grashof number (G_r), local nano particle Grashof number (B_r) and inclination (α). From Figs. 2.2 and 2.3 it is clear that, frictional force ($\bar{F}$) increases with the increase of coupling number (N), Brownian motion parameter (N_b). It is interesting to observe from Fig. 2.8 that, with the increase of slip parameter (k), frictional force ($\bar{F}$) decreases in the region $\bar{Q} \in [0, 0.8]$ and increases in the region $\bar{Q} \in [0.8, 1]$. It is also observed that frictional force ($\bar{F}$) decreases with the increase of time averaged flux ($\bar{Q}$) for fixed values of micropolar parameter (m), coupling number (N), Brownian motion parameter (N_b), thermophoresis parameter (N_t), local temperature Grashof number (G_r), local nano particle Grashof number (B_r) and inclination (α).

C. Mechanical Efficiency

Figs. 3.1-3.8 represent the effect of various parameters on mechanical efficiency (E). It is seen from Figs. 3.1, 3.2, 3.3 and 3.8 that, mechanical efficiency(E) increases with the increase of micropolar parameter (m), coupling number (N), Brownian motion parameter (N_b) and with slip parameter (k). From Figs. 3.4-3.7 it is noticed that, mechanical efficiency (E) decreases with the increase of thermophoresis parameter (N_t), local temperature Grashof number (G_r), local nano particle Grashof number (B_r) and with inclination (α). But this decrease / increase is insignificant at the lower values of time averaged flux.

D. Temperature Profile

Effects of temperature profile(θ_t) with respect to the Brownian motion parameter(N_b) and thermophoresis parameter (N_t) has been shown from Figs. 4.1-4.2. It is seen that, with the increase of Brownian motion parameter (N_b), temperature profile (θ_t) decreases and with the increases of thermophoresis parameter (N_t), temperature profile (θ_t) increases. The temperature profile (θ_t) value is minimum/maximum for $r \in [-0.5, 0.5]$.

E. Nano particle phenomenon

Figs. 5.1-5.2 explain the nature of nano particle phenomena (σ) for different values of Brownian motion parameter (N_b) and thermophoresis parameter (N_t). It is observed that, nano particle phenomena (σ)decreases with the increase of Brownian motion parameter (N_b) and increases with the thermophoresis parameter (N_t)and it reaches maximum at $r = 0$.

F. Heat Transfer Coefficient

Figs.6.1-6.3 indicate the variation of heat transfer coefficient (Z_θ) for various values of Brownian motion parameter (N_b), thermophoresis parameter (N_t) and amplitude ratio (ϵ). From Figs. 6.2-6.3, the value of the heat transfer coefficient (Z_θ)increases in the region $r \in [-1, 0]$ and decreases in the region $r \in [0, 1]$ with the increase of thermophoresis parameter (N_t) and amplitude ratio (ϵ). However, the heat transfer coefficient (Z_θ)shows an opposite behavior with respect to the Brownian motion parameter (N_b). It is interesting to observe that; heat transfer coefficient (Z_θ) converges in the region $r\epsilon[-1, 0]$ and diverges in the region$r\ \epsilon[0, 1]$.

G. Mass Transfer Coefficient

Figs. 7.1-7.3 illustrate the effect of various parameters on mass transfer coefficient (Z_σ). From Figs. 7.2-7.3 it is observed that, mass transfer coefficient (Z_σ) increases in the region $r \in [-1, 0]$ and decreases in the region $r \in [0, 1]$ with the increase of thermophoresis parameter (N_t) and amplitude ratio (ϵ). However, mass transfer coefficient (Z_σ) shows different behaviour with respect to Brownian motion parameter (N_b). It is interesting to observe that; mass transfer coefficient (Z_σ) converges in the region $r\epsilon[-1, 0]$ and diverges in the region$r\ \epsilon[0, 1]$.

H. Streamline patterns

Under certain conditions the streamlines on the center line in the wave frame of reference are found to split in order to enclose a bolus of fluid particles circulating along closed streamlines. This phenomenon is referred to as trapping, which is a characteristic of peristaltic motion. Since this bolus appears to be trapped by a wave, the bolus moves with the same speed as that of the wave. Figs. 8.1-8.9 show the streamline patterns for different parameters. The size of the trapped bolus increases with the increase of micropolar parameter (m), coupling number (N), thermophoresis parameter (N_t), local nano particle Grashof

ISSN 2394-3777 (Print)
ISSN 2394-3785 (Online)
Available online at www.ijartet.com

International Journal of Advanced Research Trends in Engineering and Technology (IJARTET)
Vol. 4, Issue 10, October 2017

number (B_r) and decreases with the increase of Brownian motion parameter (N_b), local temperature Grashof number (G_r), slip parameter (k) and with amplitude ratio (ε). It is interesting to observe that there is no significant change in the trapped bolus with respect to the inclination (α).

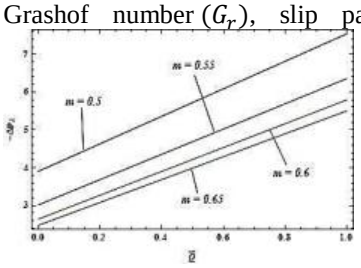

Fig. 1.1: Effect of $\bar{Q}$ and m on $(-\Delta P_\lambda)$
$(N_t = 0.8, G_r = 0.5, B_r = 0.3, \alpha = 30^0, \epsilon = 0.$
$F = 0.1, N_b = 0.3, N = 0.1, k = 0.6)$

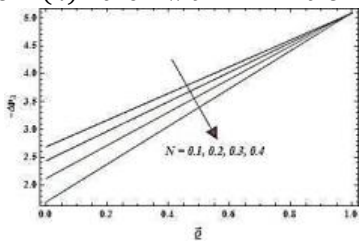

Fig. 1.2: Effect of $\bar{Q}$ and N on $(-\Delta P_\lambda)$
$(N_t = 0.8, G_r = 0.5, B_r = 0.3, \alpha = 30^0, \epsilon = 0.2,$
$F = 0.1, N_b = 0.3, m = 1.2, k = 0.8)$

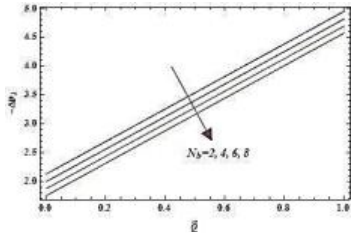

Fig. 1.3: Effect of $\bar{Q}$ and N_b on $(-\Delta P_\lambda)$
$(N_t = 0.8, G_r = 0.5, B_r = 0.3, \alpha = 30^0, \epsilon = 0.1,$
$F = 0.1, N = 0.1, m = 0.8, k = 0.6)$

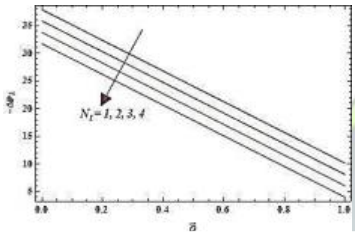

Fig. 1.4: Effect of $\bar{Q}$ and N_t on $(-\Delta P_\lambda)$
$(N_b = 0.3, G_r = 0.5, B_r = 0.3, \alpha = 30^0, \epsilon = 0.7,$
$F = 0.1, N = 0.4, m = 0.6, k = 0.6)$

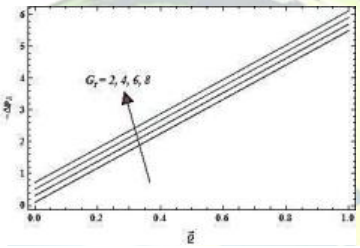

Fig. 1.5: Effect of $\bar{Q}$ and G_r on $(-\Delta P_\lambda)$
$(N_t = 0.8, N_b = 0.3, B_r = 0.3, \alpha = 30^0, \epsilon = 0.1$
$F = 0.1, N = 0.5, m = 0.9, k = 0.6)$

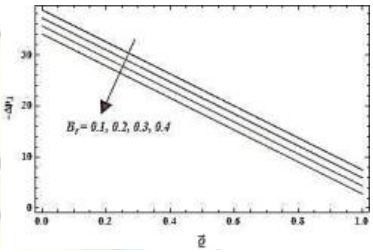

Fig. 1.6: Effect of $\bar{Q}$ and B_r on $(-\Delta P_\lambda)$
$(N_t = 0.8, N_b = 0.3, G_r = 0.5, \alpha = 30^0, \epsilon = 0.8,$
$F = 0.1, N = 0.9, m = 0.5, k = 0.6)$

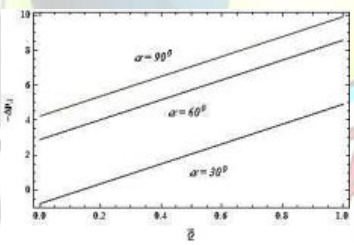

Fig. 1.7: Effect of $\bar{Q}$ and α on $(-\Delta P_\lambda)$
$(N_b = 0.3, N_t = 0.8, G_r = 0.5, B_r = 0.3, \epsilon = 0,$
$F = 0.1, N = 0.5, m = 1.2, k = 0.6)$

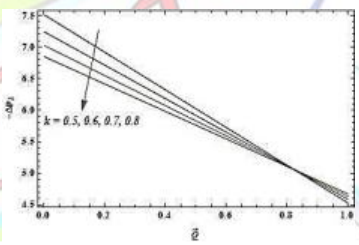

Fig. 1.8: Effect of $\bar{Q}$ and k on $(-\Delta P_\lambda)$
$(N_b = 0.3, N_t = 0.8, G_r = 0.5, B_r = 0.3, \epsilon = 0.1,$
$F = 0.1, N = 0.4, m = 1.2, \alpha = 30^0)$

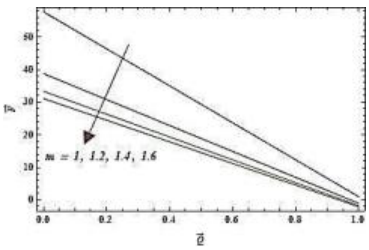

Fig. 2.1: Effect of $\bar{Q}$ and m on $\bar{F}$
$(N_b = 0.3, N_t = 0.8, G_r = 0.5, B_r = 0.3, \epsilon =$
$F = 0.1. N = 0.95. \alpha = 30^0. k = 0.6)$

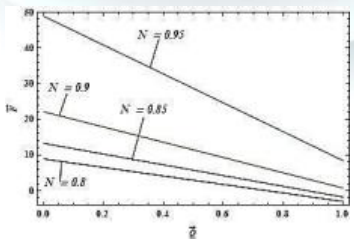

Fig. 2.2: Effect of $\bar{Q}$ and N on $\bar{F}$
$(N_b = 0.3, N_t = 0.8, G_r = 0.5, B_r = 0.3, \epsilon = 0.9,$
$F = 0.1, m = 1.5, \alpha = 30^0, k = 0.6)$

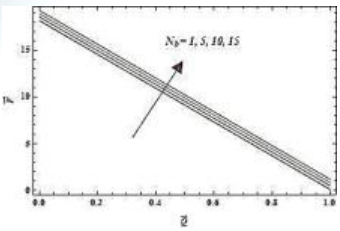

Fig. 2.3: Effect of $\bar{Q}$ and N_b on $\bar{F}$
$(N = 0.3, N_t = 0.8, G_r = 0.5, B_r = 0.3, \epsilon = 0.9,$
$F = 0.1, m = 0.9, \alpha = 30^0, k = 0.6)$

ISSN 2394-3777 (Print)
ISSN 2394-3785 (Online)
Available online at www.ijartet.com

International Journal of Advanced Research Trends in Engineering and Technology (IJARTET)
Vol. 4, Issue 10, October 2017

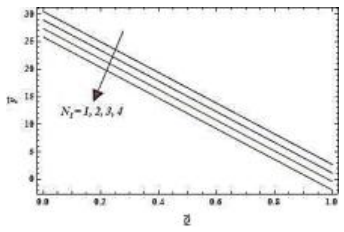

Fig. 2.4: Effect of $\bar{Q}$ and N_t on $\bar{F}$
$(N = 0.93, N_b = 0.3, \mathrm{G_r} = 0.5, \mathrm{B_r} = 0.3, \epsilon = 0.9,$
$F = 0.1, m = 1.8, \alpha = 30^0, k = 0.6)$

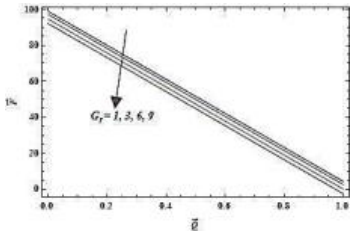

Fig. 2.5: Effect of $\bar{Q}$ and G_r on $(\bar{F})$
$(N_t = 0.6, \mathrm{N_b} = 0.3, \mathrm{B_r} = 0.3, \alpha = 30^0, \epsilon = 0.5$
$F = 0.1, N = 0.2, m = 0.9, k = 0.1)$

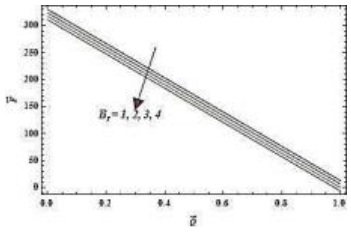

Fig. 2.6: Effect of $\bar{Q}$ and B_r on $(\bar{F})$
$(N_t = 0.9, \mathrm{N_b} = 0.3, \mathrm{G_r} = 0.5, \alpha = 30^0, \epsilon = 0.4,$
$F = 0.1, N = 0.9, m = 0.9, k = 0.2)$

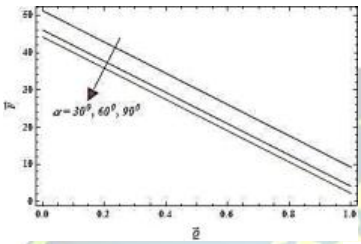

Fig. 2.7: Effect of $\bar{Q}$ and α on $(\bar{F})$
$(N = 0.9, N_b = 0.3, \mathrm{G_r} = 0.5, \mathrm{B_r} = 0.3, \epsilon = 0.9,$
$F = 0.1, m = 1.2, N_t = 0.8, k = 0.1)$

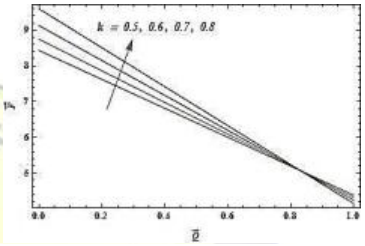

Fig. 2.8: Effect of $\bar{Q}$ and k on $(\bar{F})$
$(N_b = 0.3, N_t = 0.8, \mathrm{G_r} = 0.5, \mathrm{B_r} = 0.3, \epsilon = 0.1,$
$F = 0.1, N = 0.8, m = 1.2, \alpha = 30^0)$

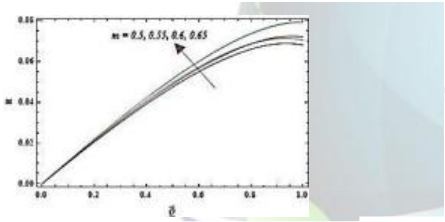

Fig. 3.1: Effect of $\bar{Q}$ and m on E
$(N_b = 0.3, N_t = 0.8, \mathrm{G_r} = 0.5, \mathrm{B_r} = 0.3, \epsilon = 0.9,$
$F = 0.1, N = 0.9, \alpha = 30^0, k = 0.4)$

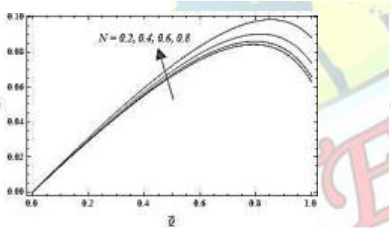

Fig. 3.2: Effect of $\bar{Q}$ and N on E
$(N_b = 0.3, N_t = 0.8, \mathrm{G_r} = 0.5, \mathrm{B_r} = 0.3, \epsilon = 0.7,$
$F = 0.1, m = 1.2, \alpha = 30^0, k = 0.2)$

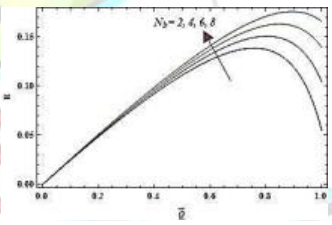

Fig. 3.3: Effect of $\bar{Q}$ and N_b on E
$(N = 0.4, N_t = 0.8, \mathrm{G_r} = 0.5, \mathrm{B_r} = 0.3, \epsilon = 0.5,$
$F = 0.1, m = 0.8, \alpha = 30^0, k = 0.3)$

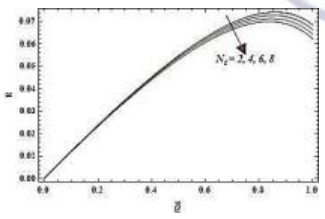

Fig. 3.4: Effect of $\bar{Q}$ and N_t on E
$(N = 0.4, N_b = 0.3, \mathrm{G_r} = 0.5, \mathrm{B_r} = 0.3, \epsilon = 0.8,$
$F = 0.1. m = 1.2. \alpha = 30^0. k = 0.6)$

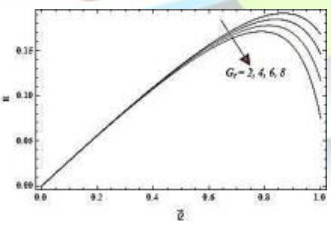

Fig. 3.5: Effect of $\bar{Q}$ and G_r on E
$(N_t = 0.8, \mathrm{N_b} = 0.5, \mathrm{B_r} = 0.3, \alpha = 30^0, \epsilon = 0.6$
$F = 0.1, N = 0.9, m = 0.8, k = 0.6)$

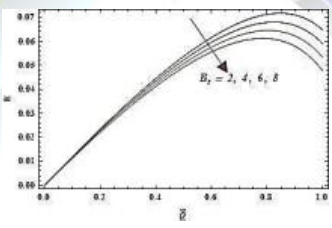

Fig. 3.6: Effect of $\bar{Q}$ and B_r on E
$(N_t = 0.8, \mathrm{N_b} = 0.3, \mathrm{G_r} = 0.5, \alpha = 30^0, \epsilon = 0.6,$
$F = 0.1, N = 0.9, m = 0.8, k = 0.6)$

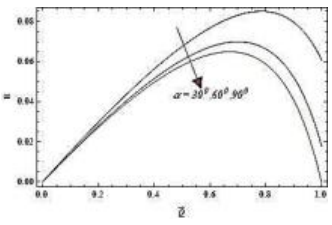

Fig. 3.7: Effect of $\bar{Q}$ and α on E
$(N = 0.8, N_b = 0.3, \mathrm{G_r} = 0.5, \mathrm{B_r} = 0.3, \epsilon = 0.7,$
$F = 0.1, m = 1.8, N_t = 0.8, k = 0.6)$

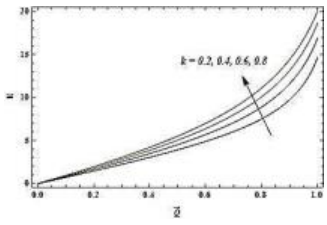

Fig. 3.8: Effect of $\bar{Q}$ and k on E
$(N_b = 0.3, N_t = 0.8, \mathrm{G_r} = 0.5, \mathrm{B_r} = 0.3, \epsilon = 0.1,$
$F = 0.1, N = 0.9, m = 1.4, \alpha = 30^0)$

ISSN 2394-3777 (Print)
ISSN 2394-3785 (Online)
Available online at www.ijartet.com

International Journal of Advanced Research Trends in Engineering and Technology (IJARTET)
Vol. 4, Issue 10, October 2017

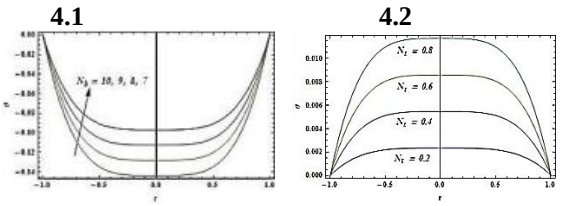

Fig. 4.1 & 4.2: Variation in Temperature profile with N_b , N_t
$(Z = 2, \epsilon = 0.9)$

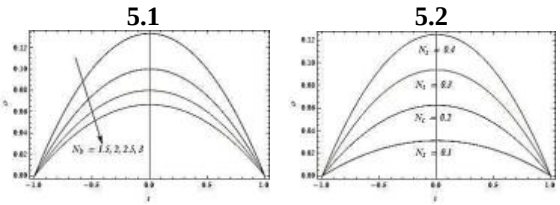

Fig. 5.1&5.2: Variation in Nano particle phenomenon with N_b, N_t
$(Z = 1, \epsilon = 0.9)$

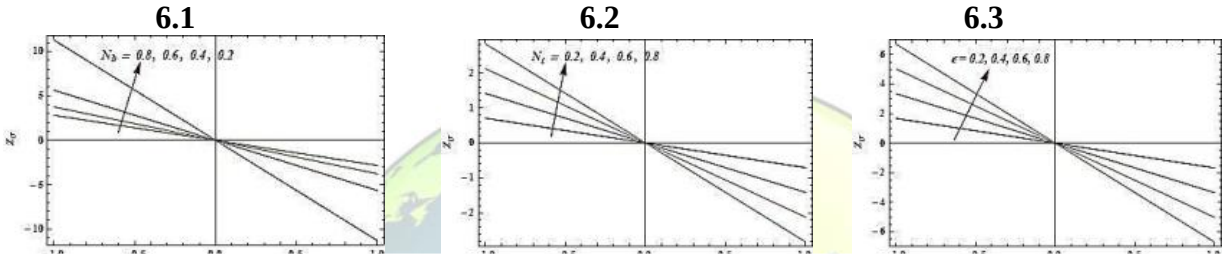

Fig. 6.1, 6.2 & 6.3: Variation in heat transfer coefficient with N_b, N_t, ϵ
$(6.1: Z = 3, \epsilon = 0.9, N_t = 0.8)(6.2: Z = 3, \epsilon = 0.9, N_b = 1.2)$ $(6.3: Z = 3, N_t = 0.8, N_b = 0.2)$

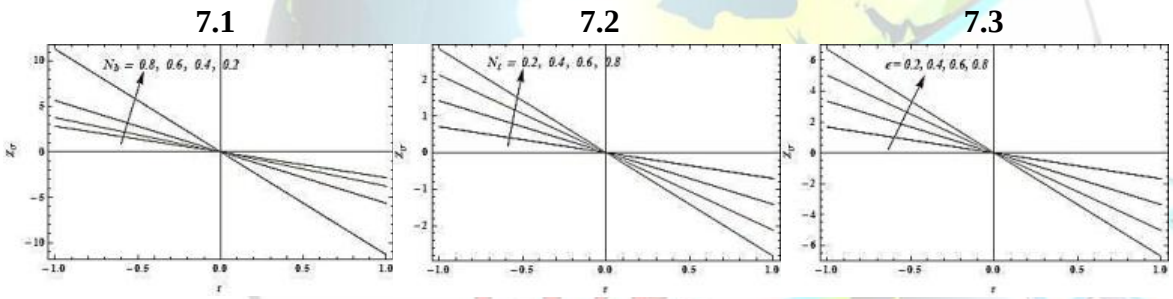

Fig. 7.1, 7.2 &7.3: Variation in Mass transfer coefficient with N_b
$(7.1: Z = 3, \epsilon = 0.9, N_t = 0.8)$ $(7.2: Z = 3, \epsilon = 0.9, N_b = 0.8)$ $(7.3: Z = 3, N_t = 0.8, N_b = 0.3)$

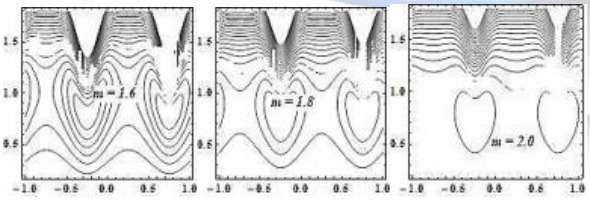

Fig. 8.1: Stream line patterns for different values of m
$\left(\epsilon = 0.5, \bar{Q} = -1.5, N = 0.8, G_r = 0.6, B_r = 0.5, \alpha = 30^0, N_b = 7, F = 0.1, k = 0.4, N_t = 3\right)$

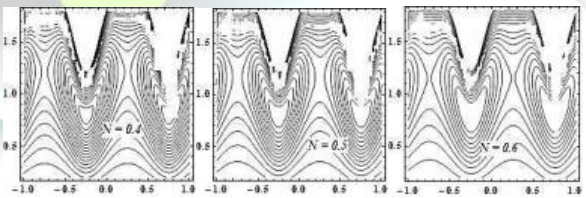

Fig. 8.2: Stream line patterns for different values of N
$\left(\epsilon = 0.5, \bar{Q} = -1.5, k = 0.4, m = 1.4, N_t = 3, B_r = 0.5, \alpha = 30^0, N_b = 7, F = 0.1, G_r = 0.6\right)$

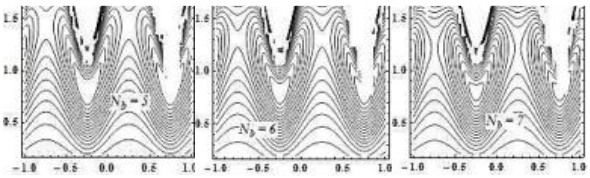

Fig. 8.3: Stream line patterns for different values of N_b
$\left(\epsilon = 0.5, \bar{Q} = -1.5, N = 0.4, m = 1.4, N_t = 3, B_r = 0.5, \alpha = 30^0, F = 0.1, k = 0.4, G_r = 0.6\right)$

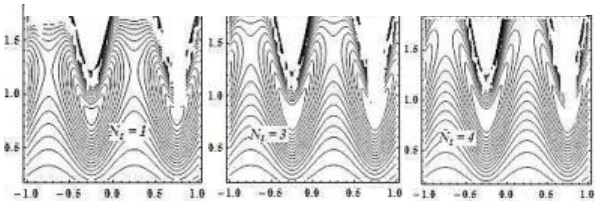

Fig. 8.4: Stream line patterns for different values of N_t
$\left(\epsilon = 0.5, \bar{Q} = -1.5, N = 0.4, m = 1.4, B_r = 0.5, \alpha = 30^0, N_b = 5, F = 0.1, k = 0.4, G_r = 0.6\right)$

ISSN 2394-3777 (Print)
ISSN 2394-3785 (Online)
Available online at www.ijartet.com

International Journal of Advanced Research Trends in Engineering and Technology (IJARTET)
Vol. 4, Issue 10, October 2017

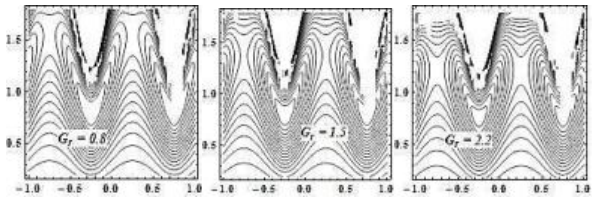

Fig. 8.5: Stream line patterns for different values of G_r
$\left(\epsilon = 0.5, \bar{Q} = -1.5, N = 0.4, m = 1.4, N_t = 4, B_r = 0.5, \alpha = 30^0, N_b = 5, F = 0.1, k = 0.4\right)$

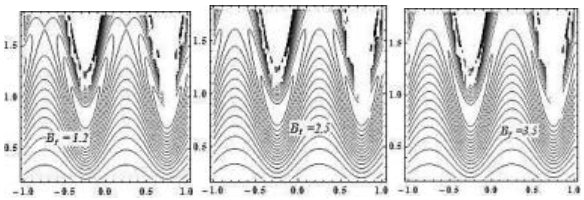

Fig. 8.6: Stream line patterns for different values of B_r
$\left(\epsilon = 0.5, \bar{Q} = -1.5, N = 0.4, m = 1.4, N_t = 4, G_r = 0.6, \alpha = 30^0, N_b = 5, F = 0.1, k = 0.4\right)$

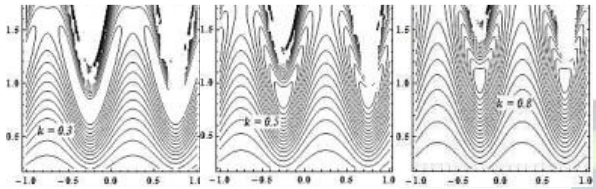

Fig. 8.7: Stream line patterns for different values of k
$\left(\epsilon = 0.5, \bar{Q} = -1.5, N = 0.4, m = 1.4, N_t = 3, B_r = 0.8, \alpha = 30^0, N_b = 5, F = 0.1, G_r = 0.6\right)$

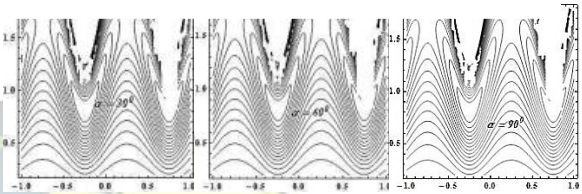

Fig. 8.8: Stream line patterns for different values of α
$\left(\epsilon = 0.5, \bar{Q} = -1.5, N = 0.4, m = 1.4, N_t = 4, B_r = 0.8, N_b = 5, F = 0.1, k = 0.4, G_r = 0.6\right)$

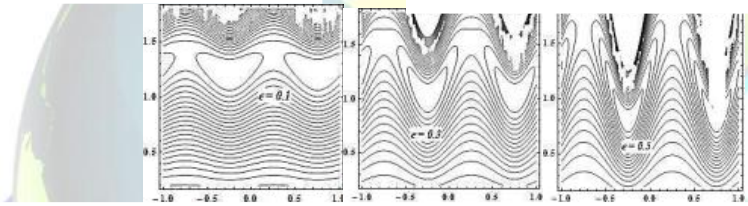

Fig. 8.9: Stream line patterns for different values of ε
$(\bar{Q} = -1.5, N = 0.4, m = 1.4, N_t = 4, B_r = 0.8, \alpha = 30^0, N_b = 5, F = 0.1, k = 0.4, G_r = 0.6)$

V. CONCLUSION

The present study is concerned with peristaltic transport of a micropolar fluid in an inclined tube with permeable walls. This study has been done with consideration to low Reynold's number and long wave length approximation. Emphasis was laid on investigating pressure rise, frictional force, mechanical efficiency, nano particle phenomenon, temperature profile, mass transfer coefficient, heat transfer coefficient and streamline patterns for the nano fluid for variables like micropolar parameter, coupling number, Brownian motion parameter, thermophoresis parameter, inclination, local temperature Grashof number and local nano particle Grashof number. Homotopy perturbation method has been used to solve the nonlinear coupled equations of temperature profile and nano particle phenomena.

The main points of the analysis are as follows:

a. The pressure rise decreases with the increase of micropolar parameter, coupling number, Brownian motion parameter, thermophoresis parameter and local nano particle Grashof number but increases with local temperature Grashof number and with inclination.
b. The pressure rise increases with the increase of time averaged flux for fixed values of micropolar parameter, coupling number, Brownian motion parameter, thermophoresis parameter, local temperature Grashof number and inclination.
c. The frictional force decreases with the increase of micropolar parameter, thermophoresis parameter, local temperature Grashof number, local nano particle Grashof number and with the inclination but increases with coupling number and Brownian motion parameter.
d. The frictional force decreases with the increases of time averaged flux for fixed values of micropolar parameter, coupling number, Brownian motion parameter, thermophoresis parameter, local temperature Grashof number, local nano particle Grashof number and inclination.
e. Mechanical efficiency increases with the increase of micropolar parameter, coupling number, Brownian motion parameter and with slip parameter but decreases with the increase of

f. thermophoresis parameter, local temperature Grashof number, local nano particle Grashof number and with the inclination.
g. The temperature profile decreases with the increase of Brownian motion parameter, increases with the increase of thermophoresis parameter and the value of the temperature profile is minimum/ maximum for $r \in [-0.5, 0.5]$.
h. Nano particle phenomenon decreases with the increase of Brownian motion parameter and increases with the increase of thermophoresis parameter and it reaches maximum at $r = 0$.
i. Heat transfer coefficient increases in the region $r \in [-1, 0]$ and decreases in the region $r \in [0, 1]$with the increase of thermophoresis parameter and amplitude ratio; and shows an opposite behaviour with the increase of Brownian motion parameter.
j. Mass transfer coefficient also increases in the region $r \in [-1, 0]$ and decreases in the region $r \in [0, 1]$with the increase of thermophoresis parameter and amplitude ratio; and shows an opposite behaviour with the increase of Brownian motion parameter.
k. The volume of the trapped bolus increases with the increase of micropolar parameter, coupling number, thermophoresis parameter and with local nano particle Grashof number but decreases with Brownian motion parameter, local temperature Grashof number, slip parameter and amplitude ratio. There is no significant change in the volume of the trapped bolus with respect to inclination.

REFERENCES

[1]. Chaube, M., Pandey, S., & Tripathi, D. (2010). Slip effect on peristaltic transport of micropolar fluid. Appl. Math. Sci, 4, 2105–2117.

[2]. Chu, W. K.-H., & Fang, J. (2000). Peristaltic transport in a slip flow. The European Physical Journal B-Condensed Matter and Complex Systems, 16(3), 543–547.

[3]. Devi, R. G., & Devanathan, R. (1975). Peristaltic motion of a micropolar fluid (Vol. 81, pp. 149–163). Presented at the Proceedings of the Indian Academy of Sciences-Section A, Springer.

[4]. Eringen, A. C. (1965). Theory of Micropolar Fluids.

[5]. Fung, Y. C., & Yih, C. S. (1968). Peristaltic Transport. Journal of Applied Mechanics, 35(4), 669–675.

[6]. Hayat, T., & Ali, N. (2008). Effects of an Endoscope on Peristaltic Flow of a Micropolar Fluid. Math. Comput. Model., 48(5-6), 721–733.

[7]. K. M. Prasad, G. R. (2009). Effect of Peripheral Layer on Peristaltic Transport of a Micropolar Fluid. Nonlinear Analysis. Modelling and Control, 1(1).

[8]. Li, M., & Brasseur, J. G. (1993). Non-steady peristaltic transport in finite-length tubes. Journal of Fluid Mechanics, 248, 129–151.

[9]. Naby, A. E. H. A. El, & Shamy, I. El. (2007). Slip effects on peristaltic transport of power-law fluid through an inclined tube. Applied Mathematical Sciences, 1(60), 2967–2980.

[10]. Nadeem, S., Riaz, A., Ellahi, R., & Akbar, N. (2014). Effects of heat and mass transfer on peristaltic flow of a nanofluid between eccentric cylinders. Applied Nanoscience, 4(4), 393–404. http://doi.org/10.1007/s13204-013-0225-x

[11]. Nicoll, P. A., & Webb, R. L. (1946). Blood Circulation in the Subcutaneous Tissue of the Living Bat's Wing. Annals of the New York Academy of Sciences, 46(8), 697–711.

[12]. Pincombe, B., Mazumdar, J., & Hamilton-Craig, I. (1999). Effects of multiple stenoses and post-stenotic dilatation on non-Newtonian blood flow in small arteries. Medical & Biological Engineering & Computing, 37(5), 595–599.

[13]. Prasad K., M., N., S., & M.A.S., S. (2015). Study of Peristaltic Motion of Nano Particles of a Micropolar Fluid with Heat and Mass Transfer Effect in an Inclined Tube. INTERNATIONAL CONFERENCE ON COMPUTATIONAL HEAT AND MASS TRANSFER (ICCHMT) - 2015, 127, 694–702.

[14]. Prasad, K. M., & Radhakrishnamacharya, G. (2009). Effect of Peripheral Layer on Peristaltic Transport of a Couple Stress Fluid. International Journal of Fluid Mechanics Research, 36(6).

[15]. Prasad, K. M., Radhakrishnamacharya, G., & Murthy, J. R. (2010). Peristaltic pumping of a micropolar fluid in an inclined tube. Int. J. of Appl. Math and Mech, 6(11), 26–40.

[16]. Prasad, K. M., Subadra, N., & Srinivas, M. (2015). Peristaltic Transport of a Nanofluid in an Inclined Tube. American Journal of Computational and Applied Mathematics, 5(4), 117–128.

[17]. Santhosh, N., Radhakrishnamacharya, G., & Chamkha, A. J. (2015). FLOW OF A JEFFREY FLUID THROUGH A POROUS MEDIUM IN NARROW TUBES. Journal of Porous Media, 18(1), 71–78.

[18]. Shapiro, A. H., Jaffrin, M. Y., & Weinberg, S. L. (1969). Peristaltic pumping with long wavelengths at low Reynolds number. Journal of Fluid Mechanics, 37(04), 799–825. http://doi.org/10.1017/S0022112069000899

[19]. Sobh, A. M. (2012). Peristaltic slip flow of a viscoelastic fluid with heat and mass transfer in a tube. Mathematical Problems in Engineering, 2012.

[20]. S. U.S. Choi, J. A. E. (1995). Enhancing thermal conductivity of fluids with nanoparticles. ASME FED. Proceedings of the ASME International Mechanical Engineering Congress and Exposition, 66.

[21]. Tuljappa, A. (n.d.). Slip effect on the peristaltic flow of a fractional second grade fluid through a cylindrical tube.